PLANT SCIENCE TODAY
Vol x(x): xx–xx
https://doi.org/10.14719/pst.10687

eISSN 2348-1900

RESEARCH ARTICLE

In vitro anticancer activity of *Passiflora incarnata* L. and *Arctium lappa* L. methanolic extracts, non-thermal plasma and iron oxide nanoparticles in HepG2 cells

Mohamed Farid[1*], Nouf A Babteen[2], Reem S Alazragi[2], Ahmed Kh El-Ghobashy[3], Mohamed M El-Danasoury[3] & Abd-Elmonsef A El-Hadary[4]

[1]Sciences Academy of Experimental Research (SAER), Scientific Society Foundation (SSF), Mansoura, Dakahlia Governorate 35516, Egypt
[2]Department of Biological Sciences, College of Science, University of Jeddah, Jeddah 21589, Saudi Arabia
[3]Department of Agricultural Biochemistry, Faculty of Agriculture, Al-Azhar University, Al-Mokhaym Al-Daem Street, Nasr City, Cairo 11241, Egypt
[4]Department of Molecular Biology, Egyptian Atomic Energy Authority, 3 Ahmed El-Zomor Street, Nasr City, Cairo 11787, Egypt

*Correspondence email - dr.mfarid2016@gmail.com

Received: 16 July 2025; Accepted: 11 November 2025; Available online: Version 1.0: 01 March 2026

Cite this article: Mohamed F, Nouf AB, Reem SA, Ahmed KE, Mohamed ME, Abd-Elmonsef AE. *In vitro* anticancer activity of *Passiflora incarnata* and *Arctium lappa* methanolic extracts, non-thermal plasma and iron oxide nanoparticles in HepG2 cells. Plant Science Today (Early Access). https://doi.org/10.14719/pst.10687

Abstract

Liver cancer is one of the most common malignancies worldwide and a major cause of cancer-related mortality. With limited treatment options, there is an urgent need to explore novel therapeutic approaches. Medicinal plants are of great importance and have demonstrated significant pharmacological potential. The objective of the present study was therefore to evaluate the anticancer effect of *Passiflora incarnata* L. and *Arctium lappa* L. leaf extracts, in comparison with non-thermal plasma and iron oxide nanoparticles. Cell viability was assessed using the MTT assay (3-[4,5-dimethylthiazol-2-yl]-2,5 diphenyl tetrazolium bromide) and protein expression of P53 and Bcl2 was analyzed by proteomic techniques, with β-actin as the loading control. The MTT assay revealed that *P. incarnata* and *A. lappa* leaf extracts reduced the cell viability of HepG2 cancer cells from 100 % to 85 % and 80 %, respectively in a dose-dependent manner (200 µL). The treatments, including leaf extracts, gliding arc plasma and nanoparticles, significantly reduced cell viability. These results were supported by genes expression of tumor-associated genes, including P53 (tumor suppressor gene) and Bcl2 (antiapoptotic gene). Non-thermal plasma treatment increased the transcription and protein expression of P53, thereby enhancing apoptotic response in the HepG2 cell line at 40, 60 and 80 sec, with corresponding viability reductions 74.33 ± 1.07 %, 82.53 ± 1.15 % and 88.05 ± 0.36 %, respectively. Regarding the effect of methanolic extracts of *P. incarnata* and *A. lappa* leaves, this study demonstrated that *P. incarnata*, *A. lappa* and iron oxide nanoparticles significantly increased P53 gene transcription, reaching 99.89 ± 0.40 %, 98.07 ± 1.08 % and 99.76 ± 1.10 %, compared with the control group (66.22 ± 2.08 %).

Keywords: extracts; genes (P53 - Bcl2 - β-actin); HepG2; nanoparticles; non-thermal plasma

Introduction

Passiflora incarnata L., commonly known as passion flower, belongs to the family Passifloraceae and is one of the most popular and widely used medicinal plants in traditional medicine in Western India, Mexico, Netherlands and South America. The plant has a long history of application in herbal medicine as an anxiolytic and sedative hypnotic which dates back to ancient time (1). *Arctium lappa* L. also known as burdock, is a plant belonging to the family Asteraceae. Previous studies have linked *A. lappa* to multiple therapeutic activities, including antitumor on human cancer cell lines. Its antioxidant activity is attributed to free-radical scavenging and oxygen-inhibitory compounds that suppress oxidative biochemical processes (2).

Nanotechnology is a multidisciplinary field, convergence of basic sciences and applied disciplines like biophysics and molecular biology. It has had a significant impact across various fields, including oncology, pulmonology and immunology, as well as in highly specialized areas such as gene delivery, tumor targeting and oral vaccine formulations (3).

Physical plasmas are composed of reactive atoms, molecules, ions and radicals. Non-thermal plasma (NTP) can produce a mixture of highly-reactive chemical species which play important roles in cell processes. At present, NTP has become a novel tool in some biomedical areas, such as sterilization, antifungal treatments, blood coagulation, dental care, wound healing and cosmetics targeted cell and tissue removal. NTP treatment has been proven effectively in inducing apoptosis *in vitro* of various tumor types and inhibiting tumor growth *in vivo*. Moreover, NTP effects on cells were dose dependent that low doses of plasma can stop cancer cells proliferation and high doses result in cell apoptosis and necrosis (4).

P53 protects cells against DNA damage-induced stresses, which could lead to transformation and tumor genesis. Mutations in

P53 have been found in over 50 % of all human tumors with loss of the gene seen in the majority of tumor types. In addition to direct loss of the P53 gene, disruption of key components in the P53 pathway have been implicated in a vast number of human tumors. Understanding the mechanisms by which P53 prevents oncogenic transformation and how these pathways are disrupted is critical for developing targeted cancer therapies (5).

Bcl2 is a family of protein responsible for dysregulation of apoptosis and prevention of death in cancer cells (6). Anti-apoptotic Bcl2 family members (Bcl-Xl) and pro-apoptotic proteins such as Bcl2-associated death protein BAD and Bcl-2-associated X protein BAX, interact to regulate pathways leading to cytochrome C release from the mitochondrial membrane. This interaction leads to Caspasace cascade activation and finally to the execution of apoptosis (7).

Materials and Methods

Plant extraction

The Sciences Academy of Experimental Researchers (SAER), located in Mansoura, Egypt, provided the *P. incarnata* and *A. lappa* leaves. The Department of Botany, Faculty of Agriculture, Al-Azhar University authenticated the plant samples. The samples were ground into a fine powder after being oven-dried at 55 °C. The powder was separated into portions for aqueous and methanolic extract production. A total of 500 g of powdered dehydrated leaves were boiled in reflux at 80 °C to 100 °C in reflux for 3 hr in 5 L distilled water to produce the aqueous extract. The extract was filtered, lyophilized and kept at 4 °C until for use (8). A total of 500 g of powdered leaves were soaked at room temperature for 8 hr in 98 % methanol (10 L) to yield a methanolic extract. The extract was stored at 4 °C, for further use. A rotating evaporator operating at 45 °C was used to concentrate it by dryness while under vacuum (9). This work was authorized by the Sciences Academy of Experimental Research's Ethics Committee in Egypt on October 28, 2024 [No. 44713].

Cell line and treatment

HepG2 (hepatocellular carcinoma) cell line obtained from the Genetic Engineering, Unit Al-Azhar University, were cultured in EMEM medium (ATCC) supplemented with 10 % fetal bovine serum (FBS, Thermo Fisher Scientific) as recommended by the supplier. Cultures were kept in a humidified 5 % CO_2 atmosphere at 37 °C and the medium was changed once a week. Tissue sampling was approved by the Clinical and Experimental Medicine and the Alazhar University Ethics Committee. The study carried out on a cell line [HepG2] a hepatocellular carcinoma (liver cancer) model. Where the cell line [HepG2] exposed to three types of treatment separately, including methanolic extract of *P. incarnata* and *A. lappa* leaves, radiation, non -thermal plasma and iron oxide nanoparticles.

Gliding arc discharge (GAD) experiment

The gliding arc (GA) is an intermediate system between thermal and non-thermal discharges and is able to provide simultaneously high plasma density, power and operating pressure with high level of non-equilibrium, high electron temperature, low gas temperature and possibility of stimulation selective chemical processes without any quenching. The main peculiarities of GA are the "memory effect" and essential influence of convective heat and mass transfer on plasma properties and the space/time arc evolution. GAD is an auto oscillating phenomenon developing between at least two electrodes that are immersed in a laminar or turbulent gas flow,

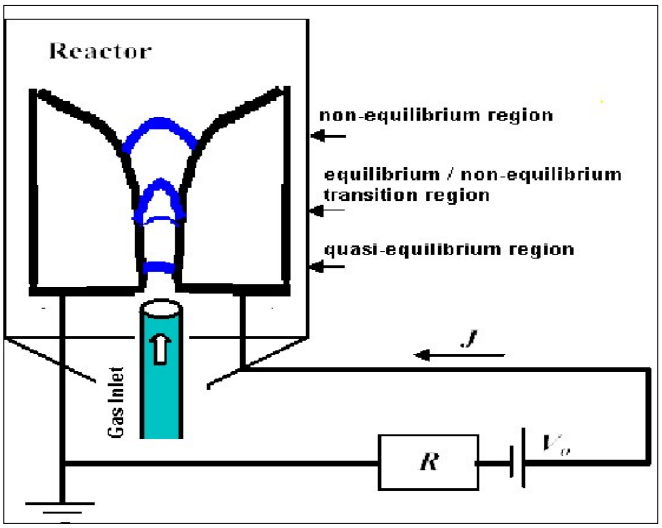

Fig. 1. Simplified scheme of the gliding arc (GA).

which provides significantly non-equilibrium plasma region at elevated power level (10, 11). The reactor used for this study derives from the gliding arc or glidarc device as illustrated in Fig. 1.

Fig. 2 shows the photographs of GA for different gas flow rate at constant discharge power. With an increase in the emission intensity increased on the upstream side. Similarly, electric discharge area increased with increasing gas flow rate on the downstream side. The positive column of the main arc discharge can be regulated by the applied discharge power. The downstream domain forms a plasma jet plume extending between the electrodes, whose behaviour depends on the gas flow rate.

The GAD for different discharge power at 60 L min^{-1} in air gas flow rate indicate that, in the upstream side, emission intensity was strong and it increased with increasing discharge voltage. In addition, electric discharge area is small and it was increased with increasing the discharge voltage. On the other hand, emission

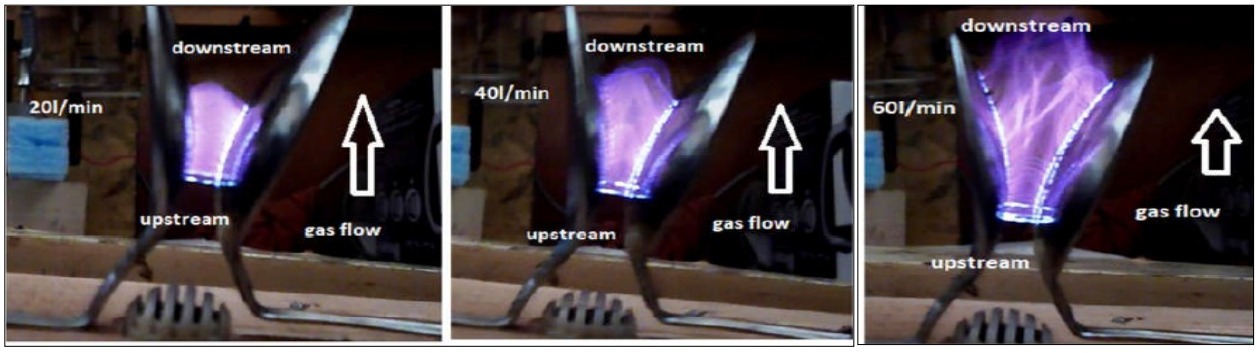

Fig. 2. Photographs of gliding arc (GA) for different gas flow rate at constant discharge voltage.

intensity is weak and electric discharge area is large in the downstream side. Although emission intensity is almost constantly independent for the discharge voltage, discharge area decreased

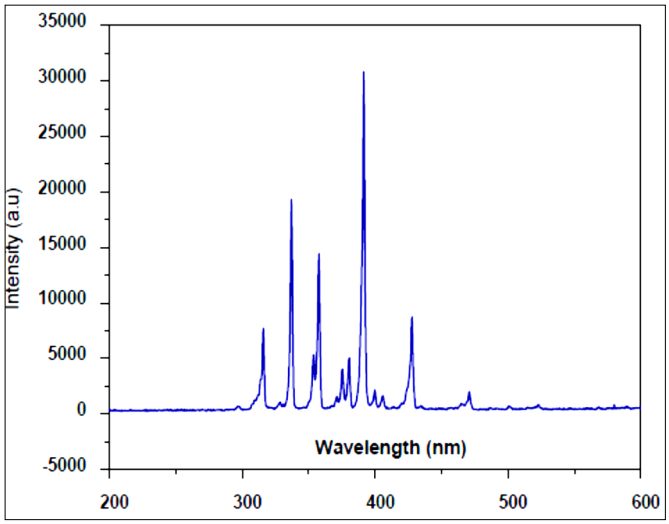

Fig. 3. Spectroscopic emission in air discharge plasma region.

with increasing discharge voltage in the downstream. The species formed in air discharge plasma region were detected with spectroscopic emission and the result has been presented in Fig. 3.

Preparation of iron oxide nanoparticle

The synthesis and characterization of iron oxide nanoparticles were carried out as follows:

Chemicals

Iron chloride ($FeCl_3$, 99 %), trisodium citrate dehydrate salt ($C_6H_5O_7.2H_2O$, 95 %), ammonium thiocyanate (NH_4SCN, 99 %), 0.05 M EDTA and methanol were purchased from Fluka. Polyethylene glycol was purchased from Sigma-Aldrich, doubled distilled water was used.

Procedures

The synthesis of hematite nanoparticles was performed as per method (12). A solution of 0.1 M $FeCl_2$ (15 mL) was added drop by drop to 100 mL of vigorously stirred boiling distilled water. The color changed from yellow ($FeCl_3$) to red and upon excess addition of 0.1 M $FeCl_3$, the color turned to dark red. The resulting solution was heated to reflux and kept at the temperature for 30 min, solution was then cooled to room temperature. The colloidal solution remained stable without visible precipitation. However, a reddish-brown precipitate was obtained upon adding excess amount of concentrated solution of ammonium phosphate tribasic tri hydrate [$(NH_4)_3 PO_{4.3}H_2O$].

The prepared iron oxide nanoparticles had an average diameter of 6 nm (60 Å), corresponding to a hydrated nanoparticle volume of 1.13×10^5 Å^3. Based on this volume, the total number of nanoparticles present in 1 L of the prepared solution was calculated to be 4.231×10^{16} particles, which is equivalent to a molar concentration of 70.28 nM. The extinction coefficient ($\varepsilon\lambda$) of the synthesized iron oxide nanoparticles was determined to be 6.8×10^7 M^{-1} cm^{-1}.

Experimental design

The HepG2 cell line was divided into seven experimental groups. Group 1 served as the untreated control. Groups 2, 3 and 4 consisted of HepG2 cells exposed to non-thermal plasma for 40, 60 and 80 sec respectively. Group 5 included cells treated with 200 µL of the methanolic extract of *P. incarnata* leaves, while Group 6 included cells treated with 200 µL of the methanolic extract of *A. lappa* leaves. Finally, Group 7 consisted of HepG2 cells treated with 200 µL of iron oxide nanoparticles (13).

After treatment, the HepG2 cell line was cultured for three days and cell viability was assessed using the MTT assay. Cytotoxicity was evaluated following the MTT protocol (Abcam MTT Cell Proliferation Kit, ab211391) (14). Briefly, HepG2 cells (1×10^5 cells/well) were seeded in 96-well plates containing 0.2 mL of medium per well. After incubation, the medium was carefully removed and the wells were washed 2-3 times with minimum essential medium (MEM) containing fetal calf serum (FCS). Subsequently, 200 µL of MTT solution (5 mg/mL) was added to each well and the plates were incubated for 6 hr–7 hr at 5 % CO_2 to allow for formazan formation. Following incubation, 1 mL of DMSO was added to each well to solubilize the formazan crystals and the contents were mixed thoroughly using a micropipette and left for 45 sec. The development of a purple color indicated the presence of viable cells. The resulting suspension was transferred to cuvettes and optical density (OD) was measured at 595 nm using DMSO as a blank. Cell viability was calculated using the formula:

Cell viability (%) = (Mean OD / Control OD) × 100

The IC_{50} value was determined graphically by plotting drug concentration on the x-axis and relative cell viability on the y-axis. In addition to viability assessment, molecular analyses were conducted. These included proteomic evaluation of P53 and Bcl2 gene expression, using β-actin as the internal control.

Blotting technique

The blotting technique was performed using standard western blot procedures. Blotting solutions included a blotting buffer composed of 25 mM Tris (pH 7.4), 0.15 M NaCl and 0.1 % Tween-20; a blocking solution consisting of 2 %–5 % nonfat dry milk prepared in blotting buffer (pH adjusted to 7.4) and an antibody solution containing 1 %–5 % non-fat dry milk in blotting buffer (pH 7.4).

Proteins separated on SDS-PAGE were transferred to a Hybond™ nylon membrane (GE Healthcare) using a TE62 standard transfer tank with cooling chamber (Hoefer Inc.). The membrane was then incubated in the blocking solution for 1 hr at room temperature, with β-actin included as a housekeeping protein. Following blocking, the membrane was incubated overnight at 4 °C in the antibody solution containing the primary anti-P53 antibody (Abcam, ab131442) and for normalization, the anti-β-actin antibody (Abcam, ab228001).

After primary antibody incubation, the membrane was washed at room temperature for 30-60 min with at least five changes of blotting buffer. It was then incubated for 1 hr at room temperature with an HRP-conjugated secondary antibody prepared in antibody solution, using a working concentration of 0.1–0.5 µg/mL (adjustable between 0.05–2.0 µg/mL for optimal signal and minimal background). Finally, the membrane was washed again for 30–60 min with multiple changes of blotting buffer. Methodological guidelines followed established references, including antibody techniques, immunochemical protocols, second edition and using antibodies: A laboratory manual (15–17).

Statistical analysis

Using the statistical software package, information collected was evaluated (18). All comparisons were first subjected to one-way ANOVA and important distinctions between treatment means were determined using Duncan multiple range test at $p < 0.05$ as the significance level (19).

Results

Antitumor activity of non-thermal plasma, methanolic extracts and iron oxide nanoparticles on cancer cell line [HepG2]: In this study determination of viability carried out through MTT assay, also molecular techniques were carried and proteomics assay of genes (P53 and Bcl2) compared with β-actin gene as standard.

The P53 gene functions as a tumor suppressor, while the Bcl2 gene represents a proto-oncogene involved in regulating cell survival. In this study, three types of treatments were evaluated for their impact on HepG2 liver cancer cells. The first treatment involved non-thermal plasma radiation, a physical approach in which cold plasma, containing reactive chemical species such as atoms, ions and radicals, along with the physical effects of the gliding arc, has recently shown promise in enhancing cancer cell death.

The second treatment utilized methanolic leaf extracts of *P. incarnata* and *A. lappa*, both known for their bioactive compounds with potential anticancer properties. The third treatment involved iron oxide nanoparticles, which were tested for their ability to induce cytotoxicity through nanoscale interactions and oxidative stress. Together, these treatments provided a comparative framework for understanding their differential effects on gene expression and cancer cell viability.

Cell viability in HepG2 cells using MTT assay

The results in Table 1 and Fig. 4, showed The percent of changes relative to normal control group. Comparing to normal control group, the levels of viability showed significant decrease in all treated group (G2–G7), at the same time. The level of changes was high significant in (G4 treated with non-thermal plasma at 80 sec). Comparison between (G2 and G3 treated with non-thermal plasma at 40 and 60 sec) and (G4 treated with non-thermal plasma at 80 sec) gives a significant decrease of G4 which means that, increasing the level of plasma dosed lead to a good treatment (Table 1; Fig. 4). The methanolic extract of *P. incarnata* and *A. lappa* leaves showed the medium values as antitumor activity of the levels of viability, which were 85.3 % and 80.2 % (G5 and G6), respectively. Compared with iron oxide nanoparticles (G7, 75.2 %).

Molecular analysis (proteomics) of gene (P53)

The results demonstrated a significant cytotoxic effect for all doses of gliding arc plasma exposure (40, 60 and 80 sec), as well as for extracts and nanoparticles (Table 1). These results supported by analysis of genes associated with tumor which were P53 as tumor suppressor gene and Bcl2 (Bcl-xl) as antiapoptotic gene. The results of P53 gene proved that, transcription of its gene and finally its protein product increased leading it increase in apoptotic effect of HepG2 cell line.

Table 1. Mean value of viability (%) of all groups

Groups	Treatment	Cell viability (%)
Group 1	Control	100.0 ± 0.00
Group 2	NTP 40 Sec	75.0 ± 1.09
Group 3	NTP 60 Sec	62.0 ± 0.17
Group 4	NTP 80 Sec	45.1 ± 0.22
Group 5	ME-PI 200 µL	85.3 ± 0.13
Group 6	ME-AL 200 µL	80.2 ± 1.12
Group 7	NIO 20 µL	75.2 ± 2.00

Group 1: control cell line, group 2, 3 and 4: treated cell line with non-thermal plasmas at 40, 60 and 80 sec, group 5: treated cell line with methanolic extracts of *P. incarnata*, group 6: treated cell line with methanolic extracts of *A. lappa*, group 7: treated cell line with iron oxide nanoparticles.

The data of molecular analysis of gene P53 and treatment effect for all groups are showed in table 2 and fig. 5. The P53 gene expression level for HepG2 cell line protein and shows increased protein production with treatments (Fig. 6a and b). The dendrogram of P53protein expression level of HepG2 cell line protein for treatments (Fig. 6c, 7-12).

Non-thermal plasma increased P53 transcription and protein levels, enhancing apoptotic in HepG2 cell line at 40, 60 and 80 sec, with expression levels of 74.33 ± 1.07 %, 82.53 ± 1.15 % and 88.05 ± 0.36 % respectively. Methanolic extracts of *P. incarnata* and *A. lappa* (groups 5 and 6) markedly increased P53 transcription compared to control, with levels of 99.89 ± 0.40 % and 98.07 ± 1.08 % respectively. Iron oxide nanoparticles (group 7) showed 99.76 ± 1.10 % P53 expression, compared to 66.22 ± 2.08 % in controls

Table 2. Data parameters of P53 protein expression level for HepG2 cell line protein with seven treatments

Groups	Treatment	Lane (%)
Group 1	Control	66.22 ± 2.08
Group 2	NTP 40 sec	74.33 ± 1.07
Group 3	NTP 60 sec	82.53 ± 1.15
Group 4	NTP 80 sec	88.05 ± 0.36
Group 5	ME-PI 200 µL	99.89 ± 0.40
Group 6	ME-AL 200 µL	98.07 ± 1.08
Group 7	NIO 200 µL	99.76 ± 1.10

Group 1: control cell line, group 2, 3 and 4: treated cell line with non-thermal plasmas at 40, 60 and 80 sec, group 5: treated cell line with methanolic extracts of *P. incarnata*, group 6: treated cell line with methanolic extracts of *A. lappa* and group 7: treated cell line with iron oxide nanoparticles.

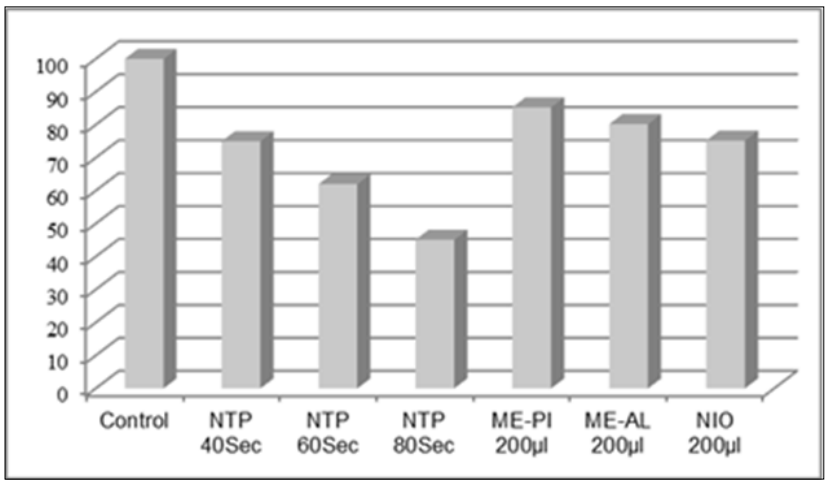

Fig. 4. Mean value of viability (%) of all groups.

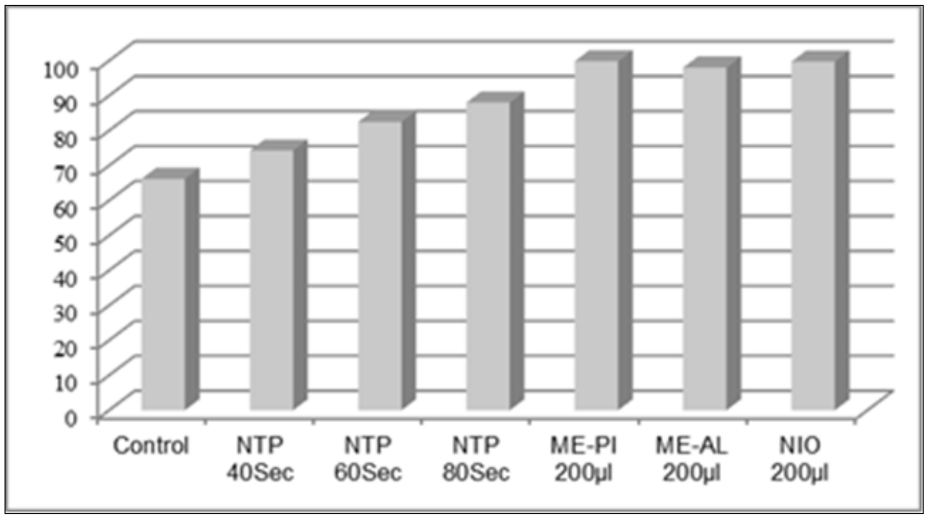

Fig. 5. P53 protein expression level of HepG2 cell line protein.

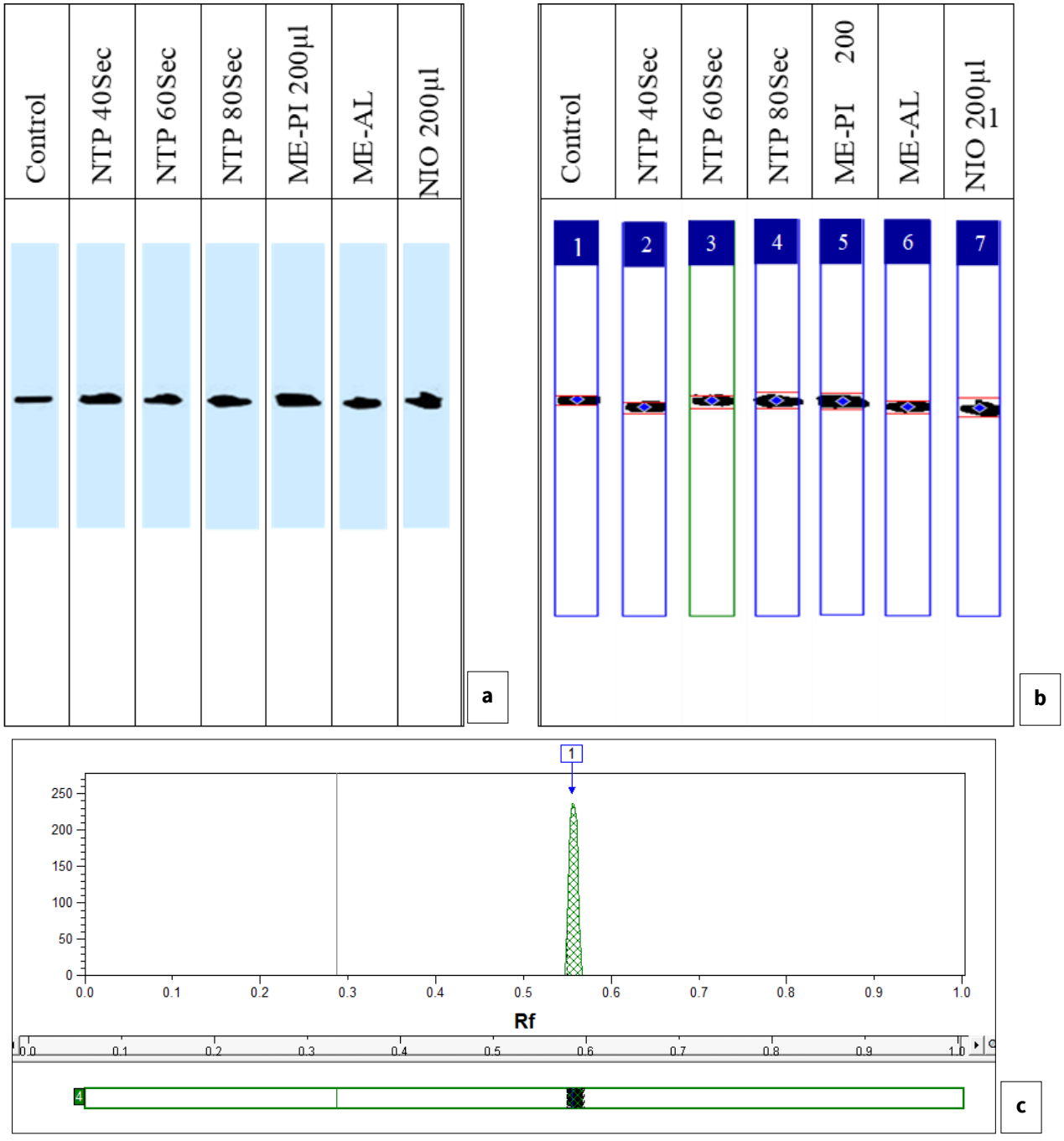

Fig. 6. (a) P53 protein expression level for HepG2 cell line protein with seven treatments; (b) Computerized detection of P53 protein expression level for HepG2 cell line protein with seven treatments; (c) Dendrogram of P53 protein expression level of HepG2 cell line protein for control.

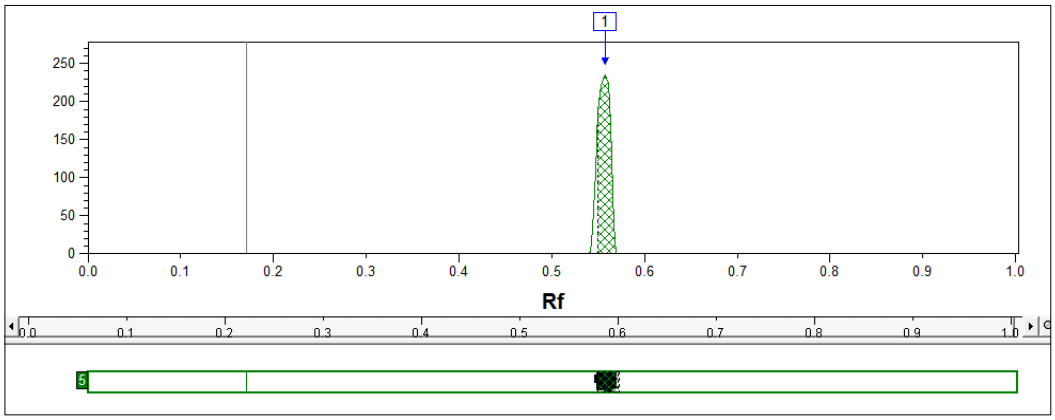

Fig. 7. Dendrogram of P53 protein expression level of HepG2 cell line protein for NTP 40 sec.

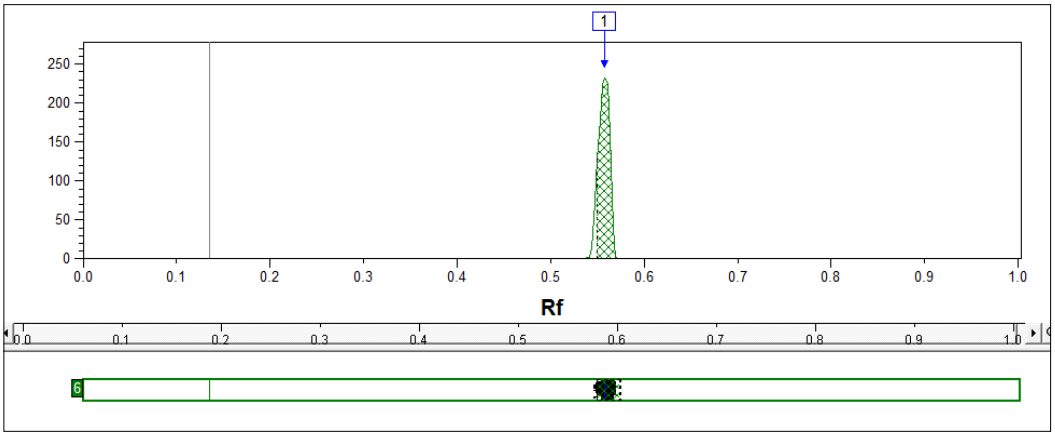

Fig. 8. Dendrogram of P53 protein expression level of HepG2 cell line protein for NTP 60 sec.

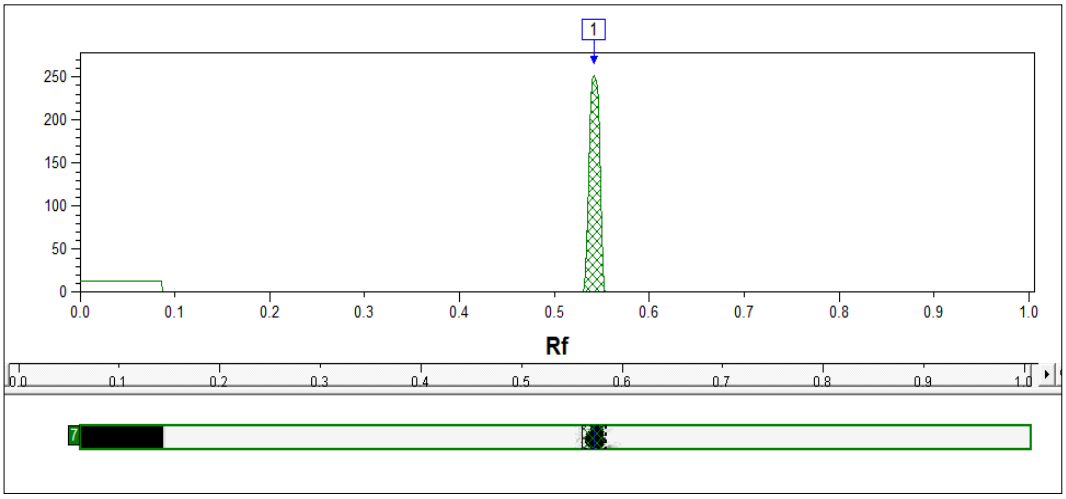

Fig. 9. Dendrogram of P53 protein expression level of HepG2 cell line protein for NTP 80 sec.

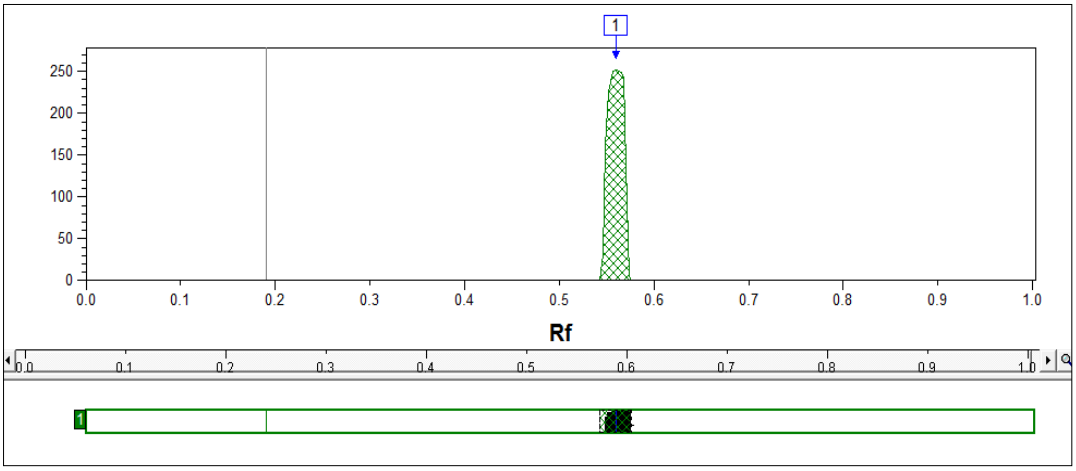

Fig. 10. Dendrogram of P53 protein expression level of HepG2 cell line protein for ME-PI 200 µL.

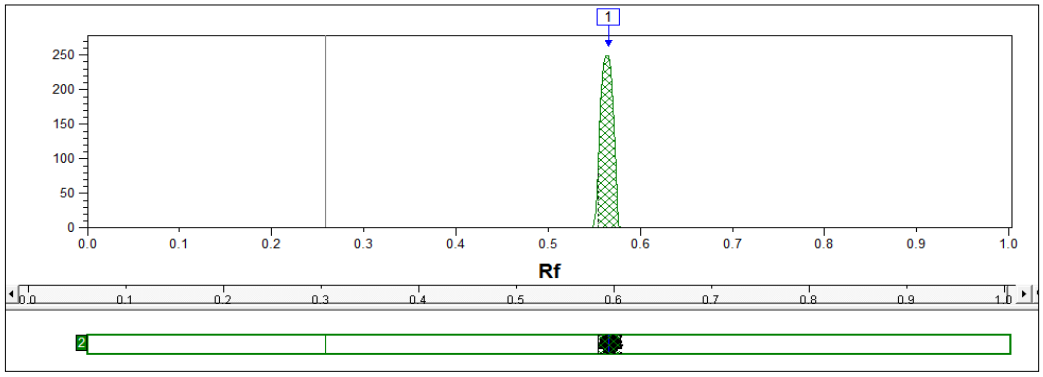

Fig. 11. Dendrogram of P53 protein expression level of HepG2 cell line protein for ME-AL 200 µL.

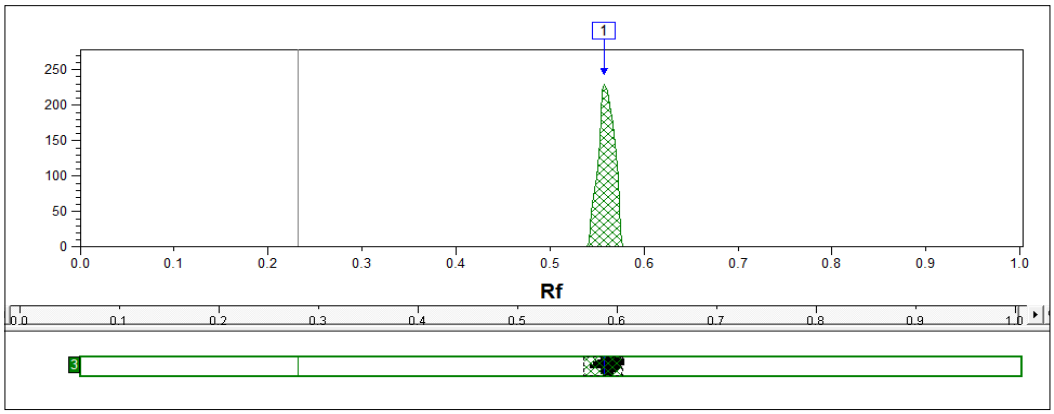

Fig. 12. Dendrogram of P53 protein expression level of HepG2 cell line protein for NIO 200 µL.

Molecular analysis (proteomics) of gene (Bcl2)

Table 3 and Fig. 13 showed the data of molecular analysis of genes (Bcl2) and treatment effects for all groups. The Bcl2 gene expression level for HepG2 cell line protein, also shows decreased protein production with treatments (Fig. 14a and b). The dendrogram of Bcl_2 protein expression level of HepG2 cell line protein for treatments (Fig. 14c, 15-20).

Non-thermal plasma it had effects on reduced transcription and protein and increases the apoptotic effect of the HepG2 cell line at 40, 60 and 80 sec, which were 72.71 ± 1.04 %, 76.54 ± 0.20 % and 67.02 ± 1.06 %, respectively. Regarding the effect of methanolic extract of *P. incarnata* and *A. lappa* leaves (group 5 and 6), high effects on reduced gene transcription Bcl2 compared control (group 1), which were 66.47 ± 0.18 % and 70.46 ± 0.15 % while the result of iron oxide nanoparticles (group 7), was 72.17 ± 1.09 %, compared with control group (86.82 ± 0.35 %).

Table 3. Data parameters of Bcl_2 protein expression level for HepG2 cell line protein with seven treatments

Groups	Treatment	Lane (%)
Group 1	Control	86.82 ± 0.35
Group 2	NTP 40 sec	72.71 ± 1.04
Group 3	NTP 60 sec	76.54 ± 0.20
Group 4	NTP 80 sec	67.02 ± 1.06
Group 5	ME-PI 200 µL	66.47 ± 0.18
Group 6	ME-AL 200 µL	70.46 ± 0.15
Group 7	NIO 20 µL	72.17 ± 1.09

Group 1: control cell line, group 2, 3 and 4: treated cell line with non-thermal plasmas at 40, 60 and 80 sec, group 5: treated cell line with methanolic extracts of *P. incarnata*, group 6: treated cell line with methanolic extracts of *A. lappa* and group 7: treated cell line with iron oxide nanoparticles.

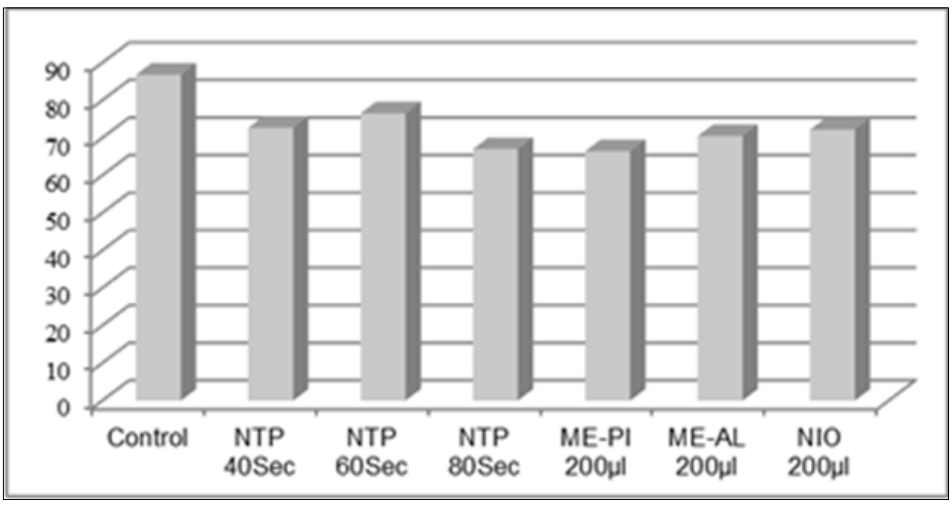

Fig. 13. Bcl_2 protein expression level of HepG2 cell line protein.

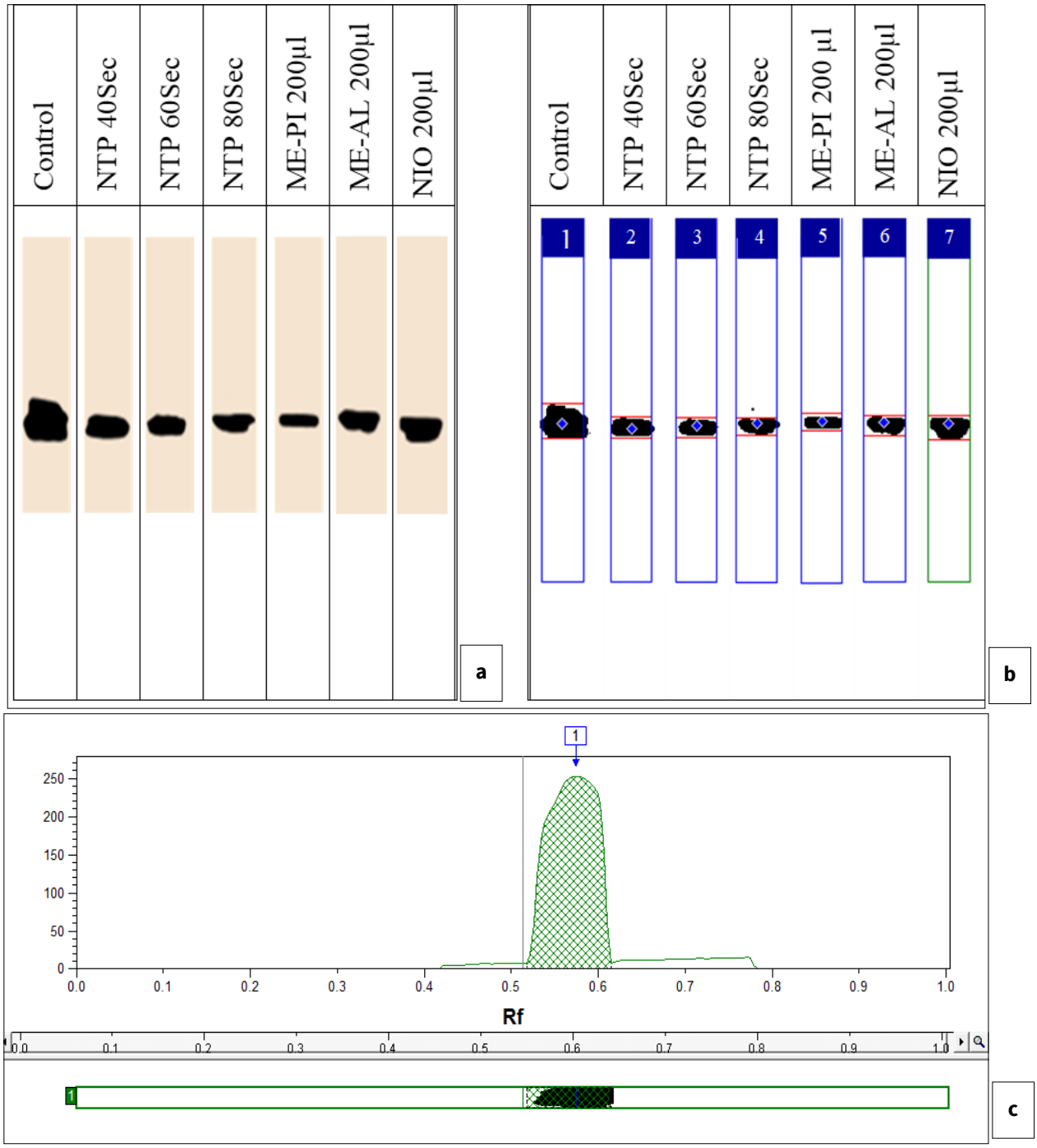

Fig. 14. (a) Bcl_2 protein expression level for HepG2 cell line protein with seven treatments; (b) Computerized detection of Bcl2 protein expression level for HepG2 cell line protein with seven treatments; (c) Dendrogram of Bcl_2 protein expression level of HepG2 cell line protein for control.

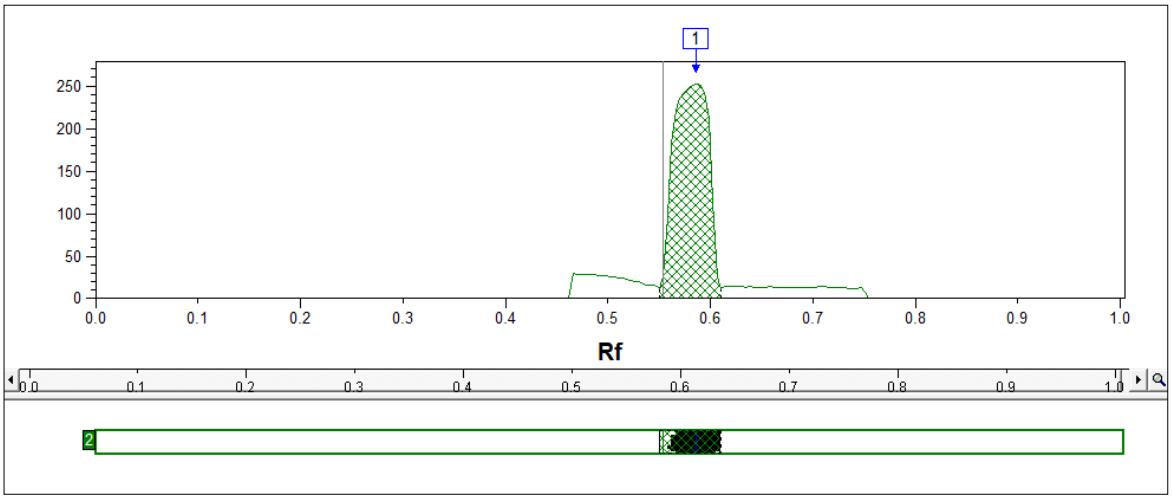

Fig. 15. Dendrogram of Bcl_2 protein expression level of HepG2 cell line protein for NTP 40 sec.

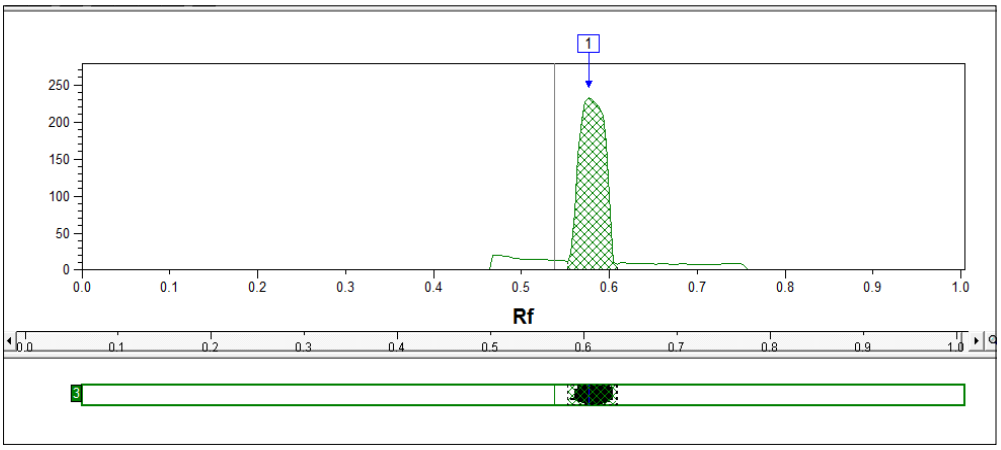

Fig. 16. Dendrogram of Bcl_2 protein expression level of HepG2 cell line protein for NTP 60 sec.

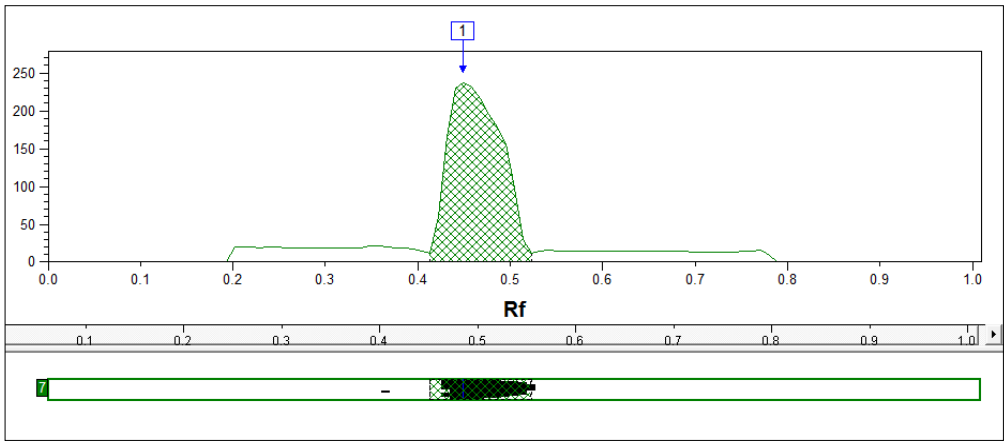

Fig. 17. Dendrogram of Bcl_2 protein expression level of HepG2 cell line protein for NTP 80 sec.

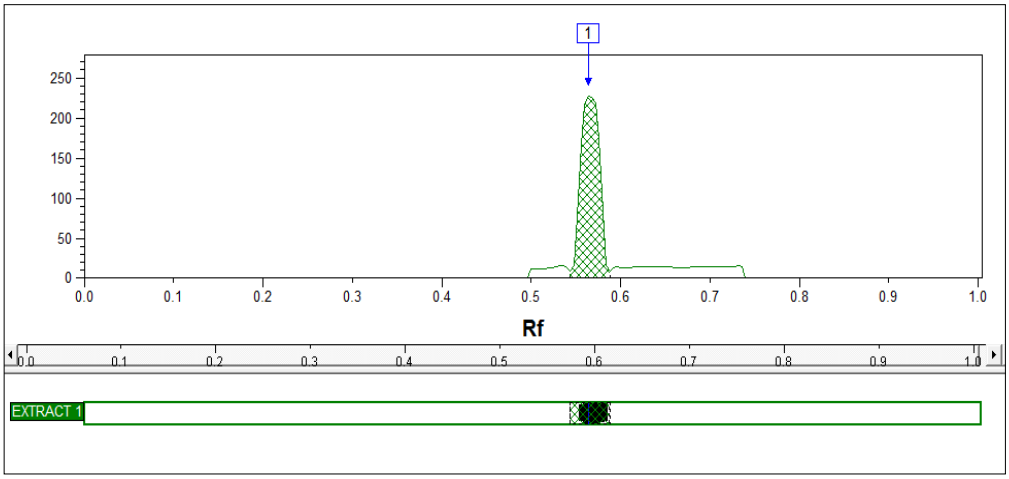

Fig. 18. Dendrogram of Bcl_2 protein expression level of HepG2 line protein for ME-PI 200 µL.

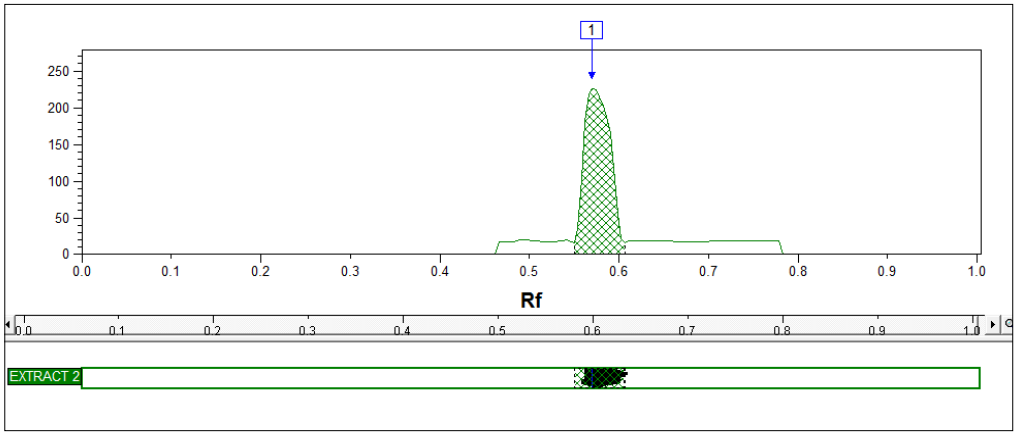

Fig. 19. Dendrogram of Bcl_2 protein expression level of HepG2 cell line protein for ME-AL 200 µL.

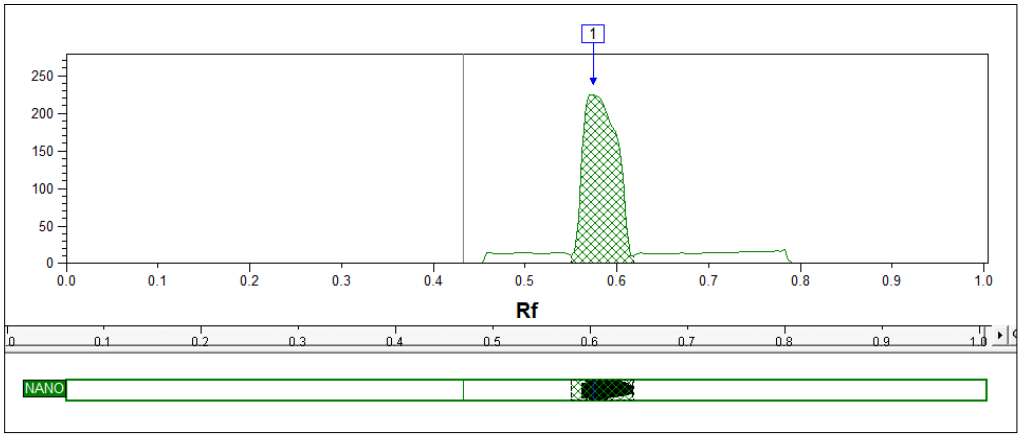

Fig. 20. Dendrogram of Bcl_2 protein expression level of HepG2 cell line protein NIO 200 µL.

Molecular analysis (proteomics) of gene (β-actin)

Actin participates in countless cellular functions ranging from organelle trafficking and pathogen motility to cell migration and regulation of gene transcription. Actin's cellular activities depend on the dynamic transition between its monomeric and filamentous forms, a process exquisitely regulated in cells by a large number of actin binding and signaling proteins (20).

The results showed that, the data of molecular analysis of genes (β-actin) and treatment effect for all groups (Table 4, Fig. 21). The β-actin gene expression level for HepG2 cell line protein, also shows convergent protein production with treatments (Fig. 22a and b). The dendrogram of β-actin protein expression level of HepG2 cell line protein for treatments (Fig. 22c, 23-28).

Table 4, β-actin results are shown when treated with Non-thermal plasma at 40, 60 and 80 sec, methanolic extract of *P. incarnata*, methanolic extract of *A. lappa* and iron oxide nanoparticles as follows 54.21 ± 0.08 %, 51.52 ± 0.02 %, 51.77 ± 0.06 %, 51.05 ± 0.11 %, 51.04 ± 0.09 % and 50.06 ± 1.09%, compared with control group (52.97 ± 0.01 %), respectively.

Molecular analysis (proteomics) of gene (β-actin)

Actin participates in countless cellular functions ranging from organelle trafficking and pathogen motility to cell migration and regulation of gene transcription. Actin's cellular activities depend on the dynamic transition between its monomeric and filamentous forms, a process exquisitely regulated in cells by a large number of actin binding and signaling proteins (20).

The results showed that, the data of molecular analysis of genes (β-actin) and treatment effect for all groups (Table 4, Fig. 21). The β-actin gene expression level for HepG2 cell line protein, also shows convergent protein production with treatments (Fig. 22a and b). The dendrogram of β-actin protein expression level of HepG2 cell line protein for treatments (Fig. 22c, 23-28).

Table 4, β-actin results are shown when treated with Non-thermal plasma at 40, 60 and 80 sec, methanolic extract of *P. incarnata*, methanolic extract of *A. lappa* and iron oxide nanoparticles as follows 54.21 ± 0.08 %, 51.52 ± 0.02 %, 51.77 ± 0.06 %, 51.05 ± 0.11 %, 51.04 ± 0.09 % and 50.06 ± 1.09%, compared with control group (52.97 ± 0.01 %), respectively.

Table 4. Data parameters of β-actin protein expression level for HepG2 cell line protein with seven treatments

Groups	Treatment	Lane (%)
Group 1	Control	52.97 ± 0.01
Group 2	NTP 40 Sec	54.21 ± 0.08
Group 3	NTP 60 Sec	51.52 ± 0. 02
Group 4	NTP 80 Sec	51.77 ± 0.06
Group 5	ME-PI 200 µl	51.05 ± 0.11
Group 6	ME-AL 200 µl	51.04 ± 0.09
Group 7	NIO 200 µl	50.06 ± 1.09

Group 1: control cell line, group 2, 3 and 4: treated cell line with non-thermal plasmas at 40, 60 and 80 sec, group 5: treated cell line with methanolic extracts of *P. incarnata*, group 6: treated cell line with methanolic extracts of *A. lappa* and group 7: treated cell line with iron oxide nanoparticles.

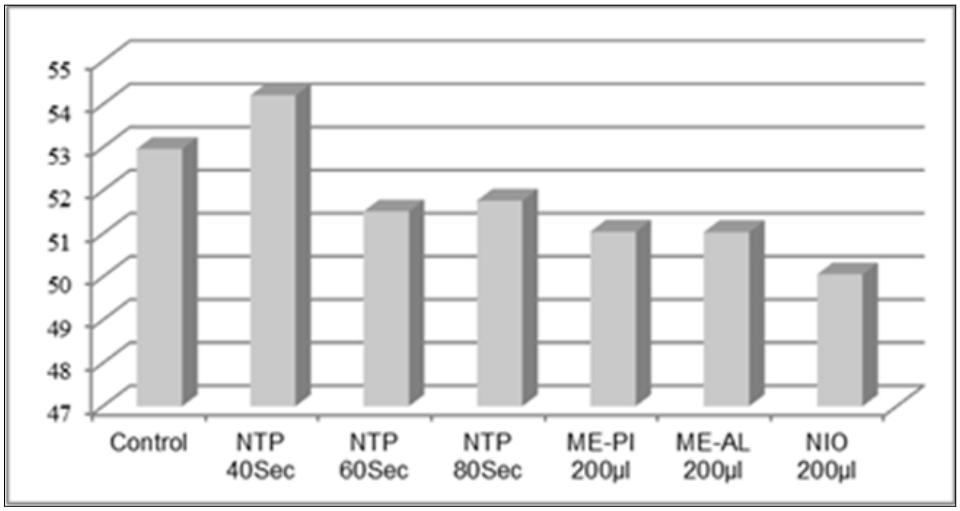

Fig. 21. β-actin protein expression level of HepG2 cell line protein.

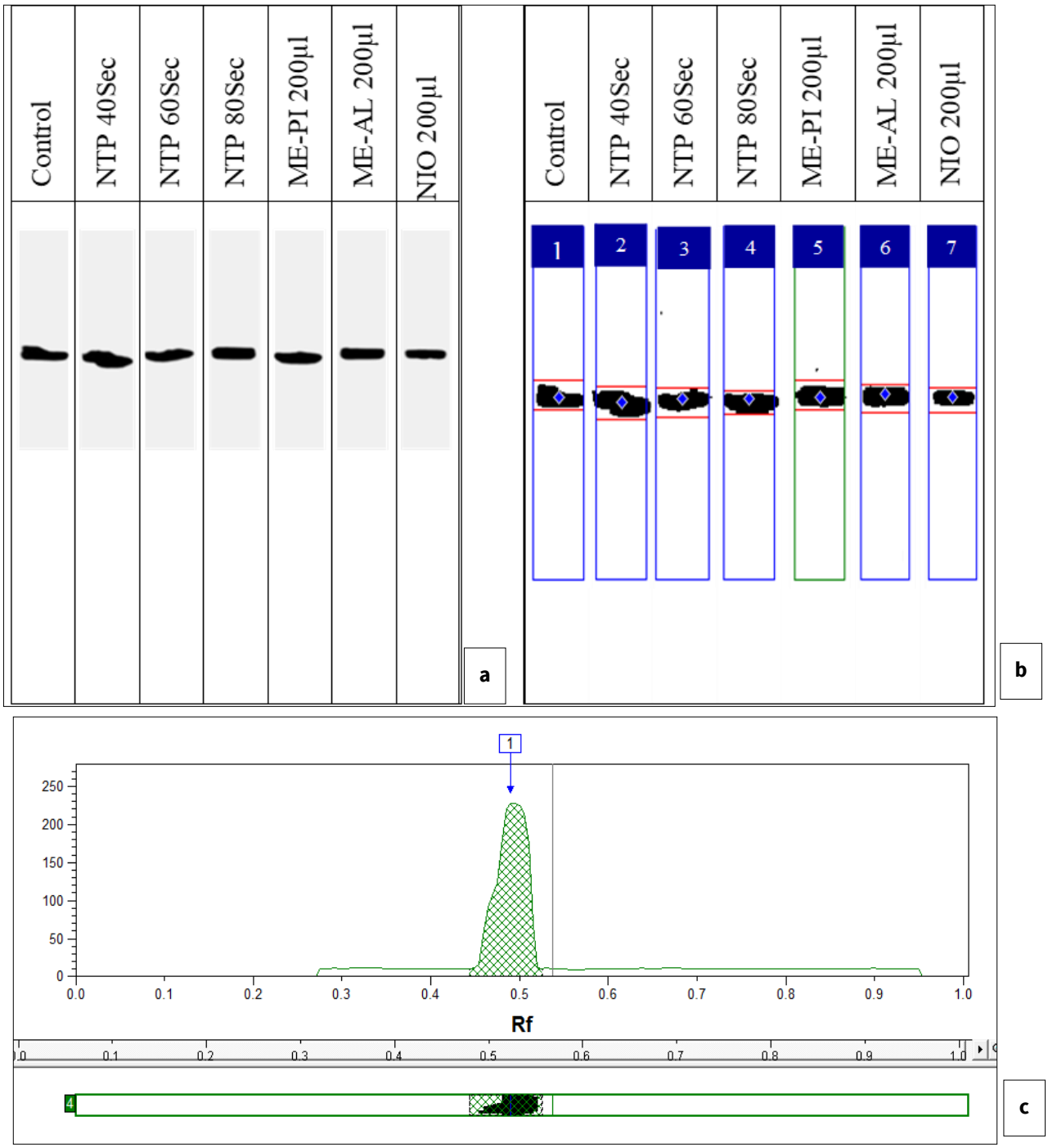

Fig. 22. (a) β-actin protein expression level for HepG2 cell line protein with seven treatments; (b) Computerized detection of β-actin protein expression level for HepG2 cell line protein with seven treatments; (c) Dendrogram of β-actin protein expression level of HepG2 cell line protein for control.

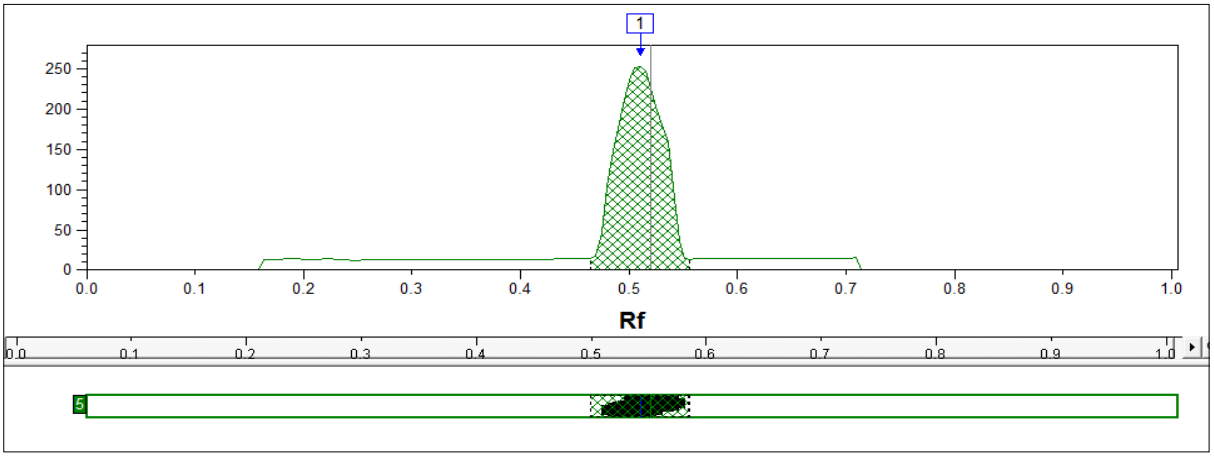

Fig. 23. Dendrogram of β-actin protein expression level of HepG2 cell line protein for NTP 40 sec.

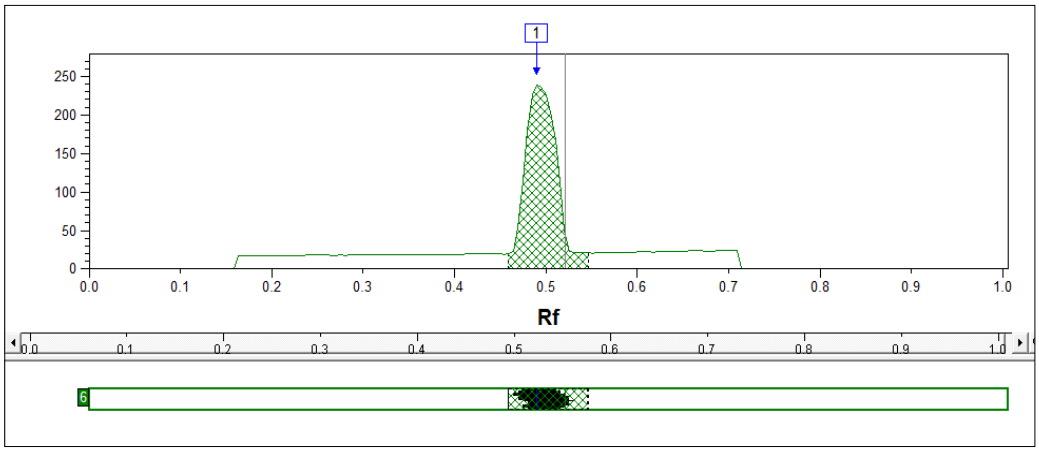

Fig. 24. Dendrogram of β-actin protein expression level of HepG2 cell line protein for NTP 60 sec.

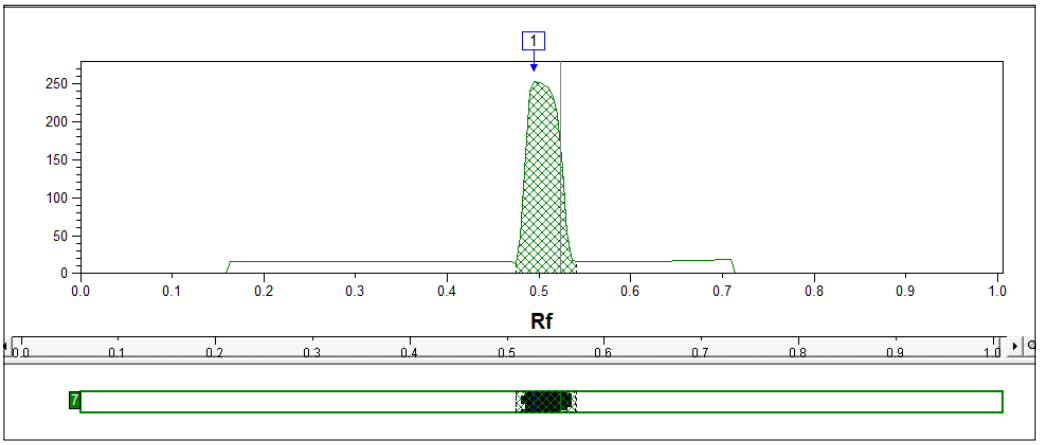

Fig. 25. Dendrogram of β-actin protein expression level of HepG2 cell line protein for NTP 80 sec.

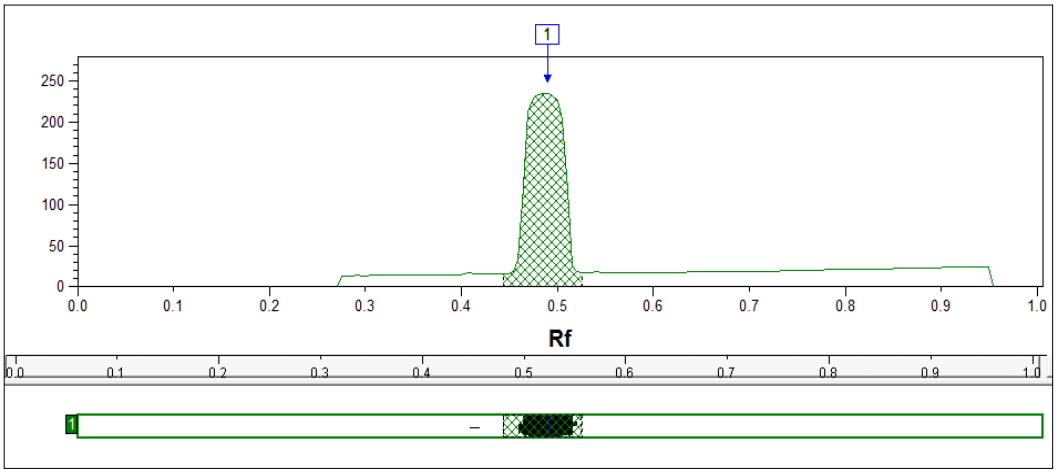

Fig. 26. Dendrogram of β-actin protein expression level of HepG2 cell line protein for ME-PI 200 µL.

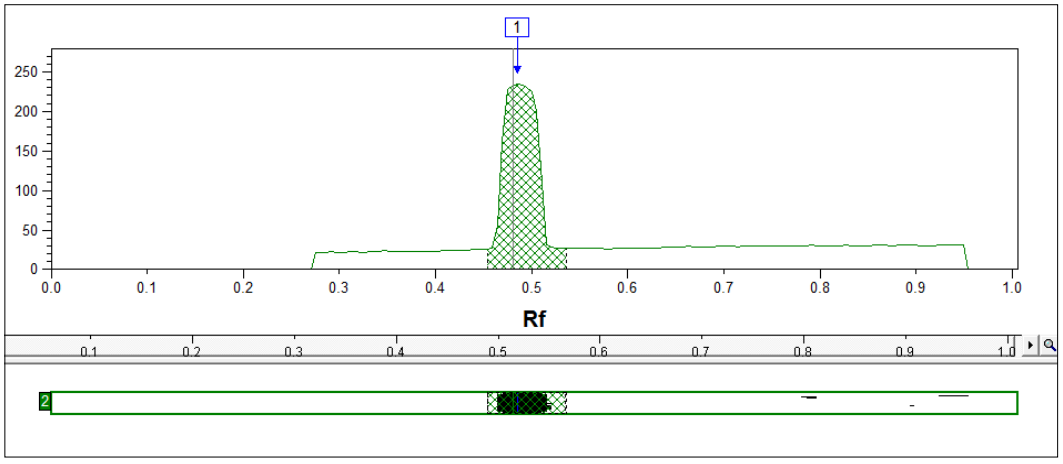

Fig. 27. Dendrogram of β-actin protein expression level of HepG2 cell line protein for ME-AL 200 µL.

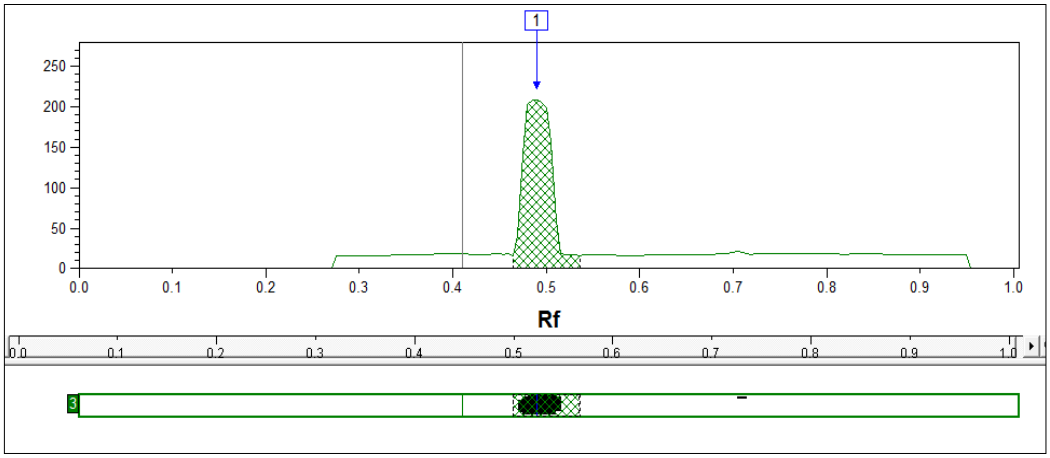

Fig. 28. Dendrogram of β-actin protein expression level of HepG2 cell line protein for NIO 200 µL.

Discussion

Passiflora caerulea extract concentrations between 1 and 150 µg/mL did not inhibit cells growth at 24 hr and 48 hr, respectively, cells viability being greater than 80 % (21). It was also observed a slight decrease in cell viability at 48 hr. At concentrations of 250 and 500 µg/mL, *P. caerulea* extract determined a decrease of cell viability after 24 hr and 48 hr respectively.

The cancer cells were treated with different concentrations of Fe_3O_4 MNPs and an MTT (3-[4,5-dimethylthiazol-2-yl]-2,5 diphenyl tetrazolium bromide) assay was used to test for cytotoxicity, resulting in an inhibitory concentra-tion 50 (IC_{50}) value of 23.83 ± 1.1 µg/mL (HepG2), 18.75 ± 2.1 µg/mL (MCF-7), 12.5 ± 1.7 µg/mL (HeLa) and 6.4 ± 2.3 µg/mL (Jurkat) 72 hr after treatment. Therefore, Jurkat cells were selected for further investigation (22).

Cell viability was examined using the MTT assay. The result showed the cell death increased by treating with nanoparticles (Fe_2O_3) in a concentration dependent manner. An increase in exposure time caused a more significant reduction in cell viability. Viability of HepG2 decreased to 12 % by giving higher dose (100 mg/mL for 24 hr) and reduced to 20 % by adding the nanoparticle in 100 mg/mL concentration for 12 hr (23).

These results are in agreement with, who mentioned that two types of cold atmospheric devices namely dielectric barrier discharge and plasma jet, show significantly anticancer capacity over dozens of cancer cell lines *in vitro*. The chrysin compound as a dietary phytochemical that is abundantly present in (*P. caerulea*), which have great economic value and medicinal impact (24). Chrysin showed a considerably increase the apoptosis of HepG2 cancer cells. The combination of chrysin and cisplatin stabilizes P53 gene expression by activating ERK1/2, which promotes P53 phosphorylation in HepG2 cells (25).

The influence of NTP on three human liver cancer cell lines (Huh7, Alexander and HepG2) at 5, 10, 15, 25, 30, 45 and 60 sec. NTP treatment resulted in higher anti-proliferative effects against Alexander and Huh7 relative to HepG2. Data showed that the NTP mediated alternation of mitochondrial membrane potential and dynamics led to reactive oxygen species (ROS) mediated apoptosis in Huh7 and Alexander cells. Interestingly, plasma treatment resulted in P53 down-regulation in Huh7 cells. High levels of Bcl-2 protein expression in HepG2 resulted in their resistance in response to oxidative stress- mediated by plasma (26).

P. edulis leaf extract contains a higher polyphenolic content, whereas in the juice extract more polysaccharide content was observed (27). On the other hand, a significant decrease in viability was observed with juice extract at 400 µg/mL and a significant increase in cytotoxicity by leaf extract at 25 µg/mL; finally, both extracts significantly increased proapoptotic activity. The treatments NTP and gemcitabine present a significant antiproliferative effect on pancreatic cells and the IC_{50}, as determined using Hill slope method, was 9 sec and 10 nM for NTP and gemcitabine, respectively. Combined treatment NTP with gemcitabine, was (5 nM) lead to an IC_{50} of 4 sec (28).

The results of present investigation exhibited that NTP and iron oxide nanoparticles treatment is higher in its effect on cell death compared to biological extracts, while on the contrary, in molecular analyzes on genes, we found that the effect of extracts is the highest impact and best treatment. This may be attributed to the ability of non-thermal plasma and iron oxide nanoparticles to penetrate cells effectively, whereas phytochemical extracts may act synergistically through secondary metabolites that mitigate oxidative damage. The results shed more light on the identification of molecular targets upon NTP treatment of liver cancer cells. Moreover, NTP as a physicochemical cue for targeted manipulation of redox signalling in the absence of other activators.

Conclusion

This study demonstrate that leaf extracts of *P. incarnata* and *A. lappa* possess significant antitumor activity in an *in vitro* liver cancer cell line (HEPG2). The results revealed that non-thermal plasma, biological extracts and iron oxide nanoparticles have effects on increased transcription and expression of the tumor suppressor gene (P53), which led to an increased apoptotic effect of the HEPG2 cell line. While the same treatments showed an effect in reducing transcription and protein output (Bcl2), which proves the efficacy of these treatments *in vitro* cancer cells inhibition and genetically treated.

Authors' contributions

MF carried out the biochemistry studies and drafted the manuscript. AAE carried out the nano and plasma assays. NAB and RSA participated in the design of the study and performed the statistical analysis. MME and AKE conceived of the study and participated in its design and coordination. All authors read and approved the final manuscript.

Compliance with ethical standards

Conflict of interest: Authors do not have any conflict of interests to declare.

Ethical issues: None

References

1. Suvarna PI, Sanjay BK. Psychopharmacological profile of *Passiflora incarnata* Linn in mice. Int J Phytopharmacol. 2012;3(3):263–8.
2. Tonea A, Oana L, Badea M, Sava S, Voina C, Ranga F, et al. HPLC analysis, antimicrobial and antifungal activity of an experimental plant based gel for endodontic usage. Stud UBB Chem. 2016;61 (4):53–68.
3. Patra AK, Das G, Fraceto LF, Campos EVR, Rodriguez-Torres MP, Acosta-Torres LS, et al. Nano based drug delivery systems: Recent developments and future prospects. J Nanobiotechnol. 2018;16:71. https://doi.org/10.1186/s12951-018-0392-8
4. Liu Y, Tan S, Zhang H, Kong X, Ding L, Shen J, et al. Atmospheric plasma on triple negative breast normal and carcinoma cells through different cell signalling pathways. Sci Rep. 2017;7:7980. https://doi.org/10.1038/s41598-017-08792-3
5. Henry H, Thomas A, Shen Y, White E. Regulation of the mitochondrial checkpoint in p53-mediated apoptosis confers resistance to cell death. Oncogene. 2002;21(5):748–60. https://doi.org/10.1038/sj.onc.1205125
6. Reed JC. Dysregulation of apoptosis in cancer. J Clin Oncol. 1999;17 (9):2941-53. https://doi.org/10.1200/JCO.1999.17.9.2941
7. Gross A, McDonnell JM, Korsmeyer SJ. BCL-2 family members and the mitochondria in apoptosis. Genes Dev. 1999;13(15):1899–911. https://doi.org/10.1101/gad.13.15.1899
8. Kim IS, Yang MR, Lee OH, Kang SN. Antioxidant activities of hot water extracts from various spices. Int J Mol Sci. 2011;12(6):4120–31. https://doi.org/10.3390/ijms12064120
9. Erian NS, Hamed HB, El-Khateeb AY, Farid M. Total polyphenols, flavonoids content and antioxidant activity of crude methanolic and aqueous extracts of some medicinal plant flowers. Arab J Sci Res Publ. 2016;2(2):53–61.
10. Fridman A, Nester S, Kennedy A, Saveliev A. Gliding arc gas discharge. Prog Energy Combust Sci. 1999;25(2):211–31. https://doi.org/10.1016/S0360-1285(98)00021-5
11. Richard F, Cormier JM, Pellerin S, Chapelle J. Physical study of a gliding arc discharge. J Appl Phys. 1996;79(5):2245–50. https://doi.org/10.1063/1.361188
12. Arndt V. Transformation of suspension of amorphous iron (III) hydroxide. IEEE Trans Magn. 1988;24:1798.
13. Indrani V, Devi PS. Evaluation of anticancer activity of *Alphonsea sclerocarpa* crude extract against HepG2 cell lines by inducing nuclear morphology changes and DNA fragmentation. J Chem Pharm Res. 2017;9(12):30–4.
14. Horiuchi N, Nakagawa K, Sasaki Y, Minato K, Fujiwara Y, Nezu K, et al. *In vitro* antitumor activity of mitomycin C derivative (RM-49) and new anticancer antibiotics (FK973) against lung cancer cell lines determined by MTT assay. Cancer Chemother Pharmacol. 1988;22 (3):246–50. https://doi.org/10.1007/BF00273419
15. Vedpal SM, Erik PL. Antibody techniques. New York: Academic Press; 1994. p. 273–89.
16. John DP. Immunochemical protocols. 2nd ed. Totowa (NJ): Humana Press; 1998. p. 207–16.
17. Harlow E, Lane D. Using antibodies: A laboratory manual. Cold Spring Harbor (NY): Cold Spring Harbor Laboratory Press; 1999. p. 267–309.
18. CoStat program. Version 6.311. Monterey (CA): Cohort Software; 2005. http://www.cohort.com
19. Duncan DB. Multiple range and multiple F tests. Biometrics. 1955;11 (1):1–42. https://doi.org/10.2307/3001478
20. Drazic A, Aksnes H, Marie M, Boczkowska M, Varland S, Timmerman E, et al. NAA80 is actin's N-terminal acetyltransferase and regulates cytoskeleton assembly and cell motility. Proc Natl Acad Sci U S A. 2018;115(17):4399–404. https://doi.org/10.1073/pnas.1718336115
21. Sesan T, Sarbu A, Smarandache D, Oancea F, Oancea A, Savin S, et al. Botanical and phytochemical approach on *Passiflora* spp. as a new nutraceutical crop in Romania. J Plant Dev. 2016;23(1):97–126. https://doi.org/10.33628/jpd.2018.25.1.3
22. Namvar F, Rahman HS, Mohamad R, Baharara J, Mahdavi M, Amini E, et al. Cytotoxic effect of magnetic iron oxide nanoparticles synthesized via seaweed aqueous extract. Int J Nanomedicine. 2014;9:2479–88. https://doi.org/10.2147/IJN.S59661
23. Sadeghi L. Cytotoxic effects of iron oxide nanoparticles on HepG2 cells. MBTJ. 2020;4(1):13–8. https://doi.org/10.22034/mbt.2020.105504
24. Yan D, Sherman JH, Keidar M. Cold atmospheric plasma, a novel promising anti-cancer treatment modality. Oncotarget. 2017;8 (9):15977–95. https://doi.org/10.18632/oncotarget.13304
25. Li X, Huang JM, Wang JN, Xiong XK, Yang XF, Zou F. Combination of chrysin and cisplatin promotes apoptosis of HepG2 cells by up-regulating p53. Chem Biol Interact. 2015;232:12–20. https://doi.org/10.1016/j.cbi.2015.03.003
26. Smolkova B, Lunova M, Lynnyk A, Uzhytchak M, Churpita O, Jirsa M, et al. Non-thermal plasma as a new physicochemical source to induce redox imbalance and subsequent cell death in liver cancer cell lines. Cell Physiol Biochem. 2019;52(1):119–40. https://doi.org/10.33594/000000009
27. Aguillon J, Arango SS, Uribe DF, Loango N. Cytotoxic and apoptotic activity of extracts from leaves and juice of *Passiflora edulis*. J Liver Res Disord Ther. 2018;4(2):67–71. https://doi.org/10.15406/jlrdt.2018.04.00102
28. Brulle L, Vandamme M, Ries D, Martel E, Robert E, Lerondel S, et al. Effects of a non-thermal plasma treatment alone or in combination with gemcitabine in a MIA PaCa2-luc orthotopic pancreatic carcinoma model. PLoS One. 2012;7(12):e52653. https://doi.org/10.1371/journal.pone.0052653

Additional information

Peer review: Publisher thanks Sectional Editor and the other anonymous reviewers for their contribution to the peer review of this work.

Reprints & permissions information is available at https://horizonepublishing.com/journals/index.php/PST/open_access_policy

Publisher's Note: Horizon e-Publishing Group remains neutral with regard to jurisdictional claims in published maps and institutional affiliations.

Indexing: Plant Science Today, published by Horizon e-Publishing Group, is covered by Scopus, Web of Science, BIOSIS Previews, Clarivate Analytics, NAAS, UGC Care, etc
See https://horizonepublishing.com/journals/index.php/PST/indexing_abstracting

Publisher information: Plant Science Today is published by HORIZON e-Publishing Group with support from Empirion Publishers Private Limited, Thiruvananthapuram, India.